



Contents lists available at ScienceDirect

# International Journal of Electronics and Communications (AEÜ)

journal homepage: [www.elsevier.com/locate/aeue](http://www.elsevier.com/locate/aeue)

## Short Communication

### A low frequency oscillator using a super-capacitor

A.S. Elwakil<sup>a,b</sup>, A. Allagui<sup>c</sup>, B.J. Maundy<sup>d</sup>, C. Psychalinos<sup>e,\*</sup><sup>a</sup> Department of Electrical and Computer Engineering, University of Sharjah, College of Engineering, P.O. Box 27272, United Arab Emirates<sup>b</sup> Nanoelectronics Integrated Systems Center (NISC), Nile University, Cairo, Egypt<sup>c</sup> Department of Sustainable and Renewable Energy Engineering, University of Sharjah, College of Engineering, P.O. Box 27272, United Arab Emirates<sup>d</sup> Department of Electrical and Computer Engineering, University of Calgary, Alberta, Canada<sup>e</sup> Department of Physics, Electronics Laboratory, University of Patras, GR-26504 Rio Patras, Greece

#### ARTICLE INFO

##### Article history:

Received 10 October 2015

Accepted 31 March 2016

Available online xxx

##### Keywords:

Low frequency oscillators

Super-capacitors

Resonance

Circuit theory

#### ABSTRACT

A low frequency relaxation oscillator is designed using a super-capacitor. An accurate analytical expression for the oscillation frequency is derived based on a fractional-order super-capacitor model composed of a resistance in series with a Constant Phase Element (CPE) whose pseudo-capacitance and dispersion coefficient are determined using impedance spectroscopy measurements. Experimental results confirm our theoretical analysis.

© 2016 Elsevier GmbH. All rights reserved.

## 1. Introduction

Low frequency oscillators are important for many applications and particularly for biomedical, electronic and instrumentation devices [1,2]. The design of such oscillators is difficult mainly due to the large values of capacitors and resistors required to achieve low oscillation frequencies [3]. Several circuit design techniques and structures have been reported in the literature to avoid the use of such impractically large component values [4–9]. However, recent developments in material science and mainly in carbon-based energy storage devices have resulted in capacitors with values exceeding 1 Farad, which are commercially available from several vendors. These capacitors are known as super-capacitors [10] and are also referred to as ultra-capacitors or electric double layer capacitors [11]. They are energy storage devices with diverse applications ranging from energy storage for wind turbines [12], and other renewable energy sources [13], hybrid and electric vehicles [14], to wireless sensor nodes [15]. The impedance of super-capacitors usually shows frequency-dependent behavior that can be modeled by a capacitance dispersion phenomena (due to distributed surface reactivity, inhomogeneity, fractal/rough geometry, and porosity) in the form of a Constant Phase Element (CPE). Thus, the most widely used model for a super-capacitor is that shown in Fig. 1 [16], which is a fractional-

order model composed of a linear resistor  $R_0$  in series with a CPE, with an impedance given by:

$$Z(s) = R_0 + \frac{1}{C_\alpha s^\alpha} \quad (1)$$

where  $C_\alpha$  is known as the “pseudo-capacitance” with units  $\text{Farad}\cdot\text{sec}^{(\alpha-1)}$  and  $\alpha$  is the dispersion coefficient ( $0 < \alpha < 1$ ). For ideal capacitive behavior,  $\alpha \approx 1$  and  $C_\alpha$  has the exact units of Farads. However, super-capacitors exhibit appreciable deviation from ideality with  $\alpha$  as low as 0.3 for some devices [17] indicating that it is incorrect to assume a behavior of a normal capacitor. Characterizing a super-capacitor requires using Electrochemical Impedance Spectroscopy (EIS) or any alternative technique such as that recently reported in [18].

In this work we investigate the possible use of a commercial super-capacitor to construct a very low frequency oscillator. To the best of the authors' knowledge such an application for super-capacitors has not yet been reported. Using the model of (1), we analytically derive an expression for the oscillation frequency. After measuring the parameter set ( $R_0, C_\alpha, \alpha$ ) using impedance spectroscopy, we clearly confirm that without using (1) and if a super-capacitor is treated as a normal capacitor based only on the vendor rating, the experimentally measured oscillation frequency cannot be explained. In particular, the rating of commercial super-capacitors is reported by vendors at DC whereas for an oscillator application, even at ultra-low frequencies, the vendor rating is insufficient to model the charge/discharge behavior of the device. This can lead to significant design errors, as will be

\* Corresponding author.

E-mail addresses: [elwakil@ieee.org](mailto:elwakil@ieee.org) (A.S. Elwakil), [aallagui@sharjah.ac.ae](mailto:aallagui@sharjah.ac.ae) (A. Allagui), [bmaundy@ucalgary.ca](mailto:bmaundy@ucalgary.ca) (B.J. Maundy), [cpsychal@physics.upatras.gr](mailto:cpsychal@physics.upatras.gr) (C. Psychalinos).

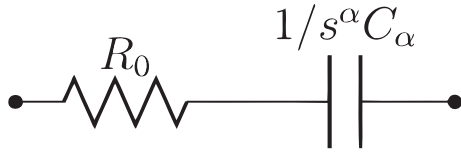


Fig. 1. Super-capacitor impedance model.

illustrated in the next sections. Furthermore, we report on the use of a super-capacitor to realize an ultra-low frequency resonance network and provide experimental results.

### 2. Low frequency oscillator

The classical and popular relaxation oscillator shown in Fig. 2 is selected. Here, we employ a 1 Farad NEC/TOKIN (Unit# FGR0H105ZF) super-capacitor device; shown within Fig. 2. According to classical analysis of the circuit, a square-wave is generated at  $V_{out}$  with a frequency  $\omega_0 = 1/RC$ , where  $R = R_1R_2/R_3$ . The super-capacitor datasheet indicates that the nominal capacitance of 1 Farad is measured at DC. If we rely on this value and select  $R_1 = 10\Omega$  with  $R_2 = R_3$ , then the expected oscillation frequency would be approximately 16 mHz. One would expect that such a very low frequency is close enough to DC and hence the datasheet value of 1 Farad can be safely adopted.

Using a Biologic VSP-300 electrochemical workstation equipped with an impedance analyzer, we measured the super-capacitor parameters using Potentiostatic Electrochemical Impedance Spectroscopy (PEIS) mode in the frequency range 10 Hz–1 kHz, with 10 points per decade, and again in the frequency range 2.5 mHz–100 mHz. From the measured data, a least-square fitting algorithm was used to estimate  $(R_0, C_\alpha, \alpha)$  according to the model of (1), as shown in Fig. 3. The same model was also used to characterize different super-capacitors in the time domain [17]. It was found that in the range 1 Hz–1 kHz,  $(R_0, C_\alpha, \alpha) \approx (7.6, 0.214, 0.29)$  which indicates that the super-capacitor is far from being an ideal capacitor. In the range 2.5 mHz–100 mHz we found  $(R_0, C_\alpha, \alpha) \approx (15.6, 0.533, 0.9)$  indicating the super-capacitor behavior is approaching that of an ideal capacitor, although  $C_\alpha$  is about half the rated value provided by the manufacturer. Based on these measurements, it would be wrong to apply the oscillation frequency expression  $\omega_0 = 1/RC$  for the circuit in Fig. 2 with a super-capacitor device. The accurate expression is derived by applying the condition

$$\left| R_0 + \frac{1}{C_\alpha(j\omega_0)^\alpha} \right| = \frac{R_1R_2}{R_3} = R \quad (2)$$

which occurs at the switching instant. Noting that

$$(j\omega_0)^\alpha = \omega_0^\alpha \left( \cos\left(\frac{\alpha\pi}{2}\right) + j \sin\left(\frac{\alpha\pi}{2}\right) \right) \quad (3)$$

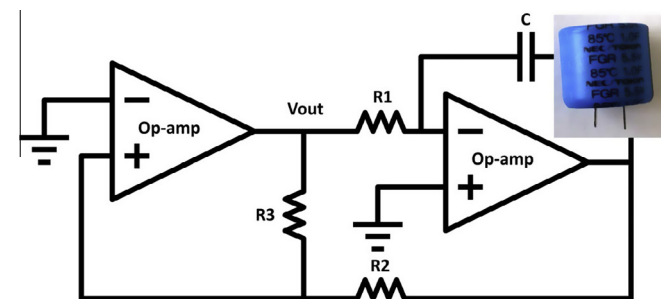


Fig. 2. Low frequency oscillator using a super-capacitor.

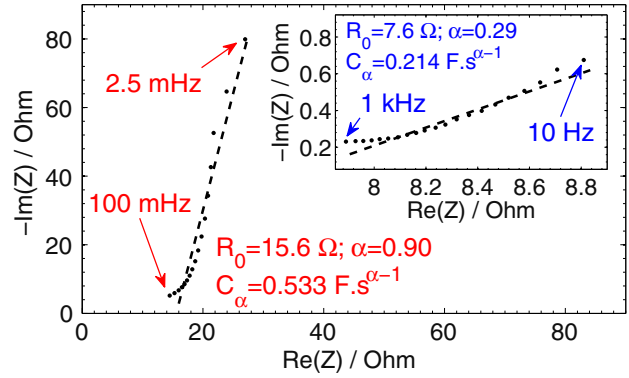


Fig. 3. Impedance spectroscopy measurement results for the 1F NEC/TOKIN super-capacitor.

we obtain

$$\left( R_0 + \frac{\cos\left(\frac{\alpha\pi}{2}\right)}{C_\alpha\omega_0^\alpha} \right)^2 + \left( \frac{\sin\left(\frac{\alpha\pi}{2}\right)}{C_\alpha\omega_0^\alpha} \right)^2 - R^2 = 0 \quad (4)$$

Solving for  $\omega_0$  yields

$$\omega_0 = \left[ \frac{R_0 \cdot \cos\left(\frac{\alpha\pi}{2}\right)}{C_\alpha \cdot (R^2 - R_0^2)} \left( 1 + \sqrt{1 + \frac{R^2 - R_0^2}{R_0^2 \cdot \cos^2\left(\frac{\alpha\pi}{2}\right)}} \right) \right]^{1/\alpha} \quad (5)$$

with the constraint  $R > R_0$ . It is clear from (5) that  $\omega_0$  is very sensitive to the difference term  $(R^2 - R_0^2)$ . For  $R^2 \gg R_0^2$ , (5) simplifies to

$$\omega_0 = (1/RC_\alpha)^{1/\alpha} = (1/RC)|_{\alpha=1} \quad (6)$$

as expected. It is important to note here that super-capacitors of the same rating and from the same vendor may have appreciable differences in their model parameters. It is thus recommended to accurately obtain a model for the super-capacitor physically being employed, either using Impedance spectroscopy or any other technique [18].

### 3. Experimental verification

The circuit in Fig. 2 was tested with TL081 op amps and  $R_2 = R_3 = 1 \text{ k}\Omega$ . At  $R_1 = 10 \Omega$ , the observed waveform is shown in Fig. 4(a) with a measured frequency of 1.38 Hz. Using (5) with the measured impedance spectroscopy values of  $(R_0, C_\alpha, \alpha) \approx (7.6, 0.214, 0.29)$  yields the very close value  $f_0 = \omega_0/2\pi = 1.42 \text{ Hz}$ . A 50  $\Omega$  resistor was then placed in parallel with the 10  $\Omega$  yielding  $R_1 \approx 8.3 \Omega$ . As predicated by (5),  $\omega_0$  increases significantly when  $R_1$  approaches  $R_0$  and we measured a frequency of 114 Hz close enough to the 137 Hz indicated by (5), as shown in Fig. 4(b). Finally, we used  $R_1 = 50 \Omega$ . With  $\omega_0$  expected to be in the mHz range, due to the large of  $R_1$ , we used the impedance spectroscopy measurements in this frequency range  $(R_0, C_\alpha, \alpha) \approx (15.6, 0.533, 0.9)$ . Accordingly, (5) indicates a 4.9 mHz waveform frequency while we observed an oscillation frequency of 12.4 mHz, as shown in Fig. 4(c). The difference between the theoretical value and the measured one is attributed to the heavy loading effect of the super-capacitor (as it approaches its near-ideal capacitive behavior with  $\alpha \approx 0.9$ ) on the op amp. This loading effect increases the op amp output resistance which can no longer be ignored. This output resistance adds up to the super-capacitor resistance  $R_0$  making it effectively higher. From (5) and substituting with  $R_0 = 40 \Omega$  instead of 15.6  $\Omega$  leads to an oscillation frequency of 9.5 mHz while substituting with  $R_0 = 45 \Omega$  leads to a frequency of 14.8 mHz meaning that the op amp output resistance is between 25  $\Omega$  and 30  $\Omega$ . The loading effect can also be

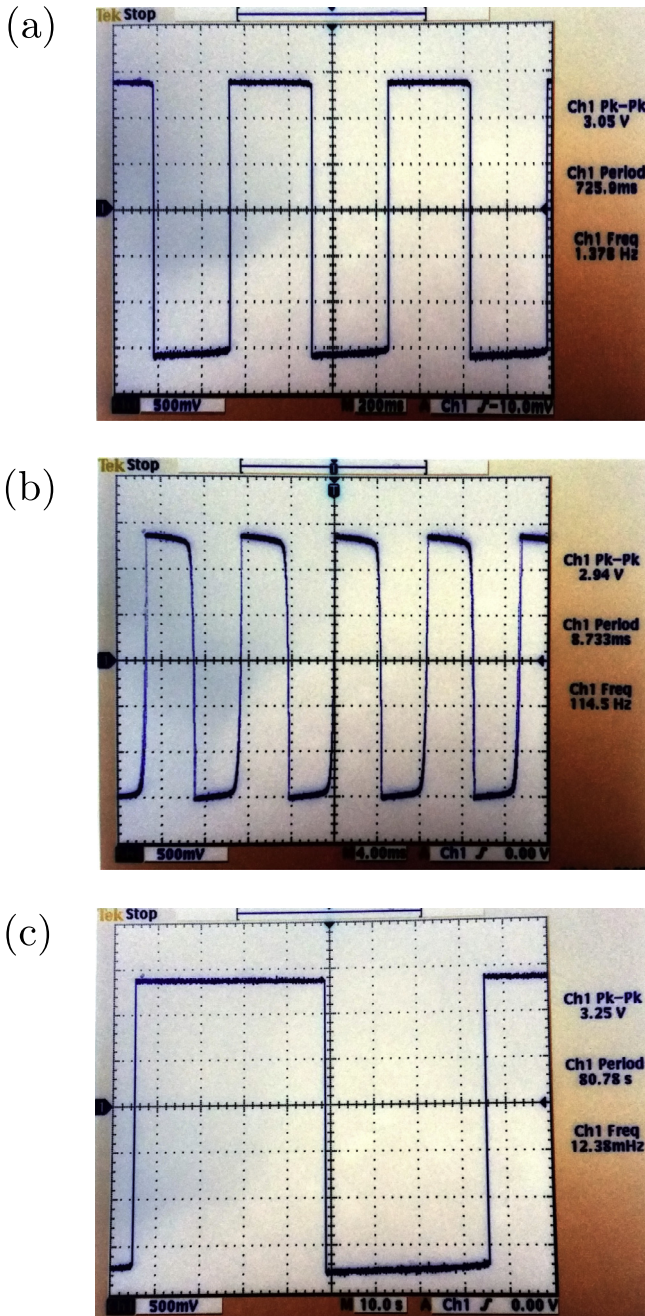


Fig. 4. Experimental results of the low frequency oscillator at (a) 1.4 Hz ( $R_1 = 10 \Omega$ ), (b) 114 Hz ( $R_1 \approx 8.3 \Omega$ ) and (c) 12.4 mHz ( $R_1 = 50 \Omega$ ).

clearly seen in Fig. 4(c) as the amplitude of the output signal has increased to 3.25 V compared to 3.05 V in Fig. 4(a) at 1.38 Hz, and 2.95 V in Fig. 4(b) at 114 Hz. In conclusion, the loading effect of super-capacitors on op amps, which increases significantly at very-low frequencies, should not be ignored.

#### 4. Low frequency resonance

In this section, we further investigate the use of a super-capacitor to obtain an ultra-low frequency series resonance network composed of an ideal inductor  $L$  and a super-capacitor. It was shown in [19,20] that the general formula for the resonance frequency  $\omega_r$ , assuming a fractional-order capacitor whose impedance is  $(C_\alpha s^\alpha)^{-1}$  and a fractional-order inductor whose impedance is  $(L_\beta s^\beta)$ , is given by

$$\omega_r = \left( \frac{\sin(\alpha\pi/2)}{\sin(\beta\pi/2)} \frac{1}{L_\beta C_\alpha} \right)^{\frac{1}{\alpha-\beta}} \quad (7)$$

Note that we may use the definition of  $C_{eff} = C_\alpha \frac{\omega^{(\alpha-1)}}{\sin(\alpha\pi/2)}$  and further define an effective inductance  $L_{eff} = L_\beta \frac{\sin(\beta\pi/2)}{\omega^{(1-\beta)}}$  in which case (7) reduces to the well-known expression

$$\omega_r = 1/\sqrt{L_{eff}C_{eff}} \quad (8)$$

Both  $C_{eff}$  and  $L_{eff}$  are in proper Farad and Henry units whereas  $C_\alpha$  and  $L_\beta$  are pseudo-capacitance and pseudo inductances in units Farad $\cdot$ sec $^{(\alpha-1)}$  and Henry $\cdot$ sec $^{(1-\beta)}$  respectively.

Here, we use three different ideal inductors ( $\beta = 1$ ) of values 1 mH, 15 mH and 100 mH to test and measure the resonance frequency when these inductors are respectively connected in series with the 1 Farad NEC/TOKIN super-capacitor characterized earlier in Section 2. Accordingly, (7) in this case reads as

$$\omega_r = \left( \frac{\sin(\alpha\pi/2)}{LC_\alpha} \right)^{\frac{1}{\alpha-1}} \quad (9)$$

With the earlier measured values of  $C_\alpha$  and  $\alpha$ , (9) indicates a resonance frequency of 57.65 Hz, 7.18 Hz and 1.67 Hz respectively for the 1 mH, 15 mH and 100 mH inductors. In Fig. 5(a) we show the Nyquist plot of the measured impedance in the three cases indicating that the imaginary part of the impedance does vanish ( $Im(Z) = 0$ ); i.e. resonance exists. Fig. 5(b) shows the phase Bode plot from which the resonance frequencies were respectively measured to be 63 Hz, 7 Hz and 2 Hz, close enough to the calculated values based on (9).

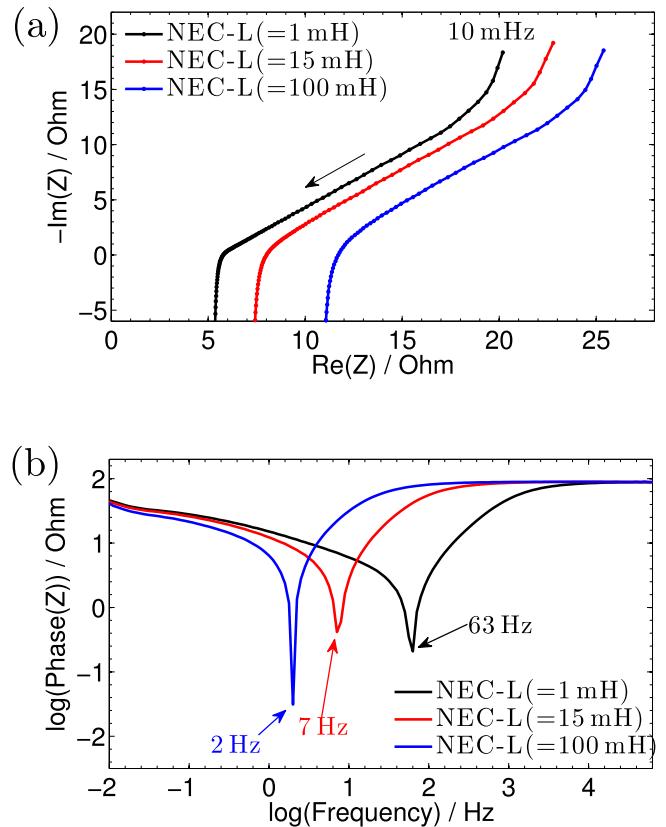


Fig. 5. Experimental results of the low-frequency resonance network using a super-capacitor and three different inductors; (a) Nyquist plot of the impedance and (b) Bode-plot of the phase.

## 5. Conclusion

The design of low frequency oscillators using super-capacitors is possible yet challenging. The rated datasheet capacitance value does not enable accurate calculation of the expected frequency. An electrochemical station, or an alternative technique [18], must be used to extract the pseudo-capacitance and more importantly the dispersion coefficient of a super-capacitor within the targeted frequency band of interest. The loading effect of supercapacitors increases at low frequencies and should also be taken into consideration.

## References

- [1] Hwang C, Bibyk S, Ismail M, Lohiser B. A very low frequency, micropower, low voltage CMOS oscillator for noncardiac pacemakers. *IEEE Trans Circ Syst I* 1995;42(11):962–6.
- [2] Wang M, Saavedra CE. Very low frequency tunable signal generator for neural and cardiac cell stimulation. *Int J Electron* 2011;98(9):1215–27.
- [3] Miyazaki T, Lim S, Minamitake C, Takeishi. Ultralow-frequency oscillator with switched capacitors. *Electron Comm Jpn Pt II Electron* 1992;75:98–106.
- [4] Elwakil AS. Systematic realization of low-frequency oscillators using composite passive–active resistors. *IEEE Trans Instrum Meas* 1998;47:584–6.
- [5] Elwakil AS, Soliman AM. Wien oscillators using current conveyors. *Comput Electr Eng* 1999;25:45–55.
- [6] Bahskar DR, Senani R. New CFOA-based single-element-controlled sinusoidal oscillators. *IEEE Trans Instrum Meas* 2006;6(55):2014–21.
- [7] Elwakil AS, Ozoguz S. A low frequency oscillator structure. In: *Europ. conf. circuit theory and design, Antalya, Turkey*. p. 588–90.
- [8] Lahiri A. Low-frequency quadrature sinusoidal oscillators using current differencing buffered amplifiers. *Indian J Pure Appl Phys* 2011;49(6):423–8.
- [9] Srivastava DK, Singh VK, Senani R. New very low frequency oscillator using only a single CFOA. *Am J Electr Electron Eng* 2015;3(1):1–3.
- [10] Mahon PJ, Paul GL, Keshishian SM, Vassallo AM. Measurement and modeling of the higher-power performance of carbon-based super-capacitors. *J Power Sources* 2000;91(1):68–76.
- [11] Kotz R, Carlen M. Principles and applications of electrochemical capacitors. *Electrochim Acta* 2000;45(15–16):2483–98.
- [12] Jayasinghe SD, Vilathgamuwa DM. Flying super-capacitors as power smoothing elements in wind generation. *IEEE Trans Ind Electron* 2013;60(7):2909–18.
- [13] Pegueroles-Queral J, Bianchi FD, Gomis-Bellmunt O. A Power smoothing system based on super-capacitors for renewable distributed generation. *IEEE Trans Ind Electron* 2014;62(1):343–50.
- [14] Cao J, Emadi A. A new battery/ultracapacitor hybrid energy storage system for electric, hybrid, and plug-in hybrid electric vehicles. *IEEE Trans Power Electron* 2012;27(1):122–32.
- [15] Kim S, No K, Chou P. Design and performance analysis of supercapacitor charging circuits for wireless sensor nodes. *IEEE J Emerging Sel Top Circuits Syst* 2011;1(3):391–402.
- [16] Martynyuk V, Ortigueira M. Fractional model of an electrochemical capacitor. *Signal Process* 2015;107(2):355–60.
- [17] Freeborn TJ, Maundy B, Elwakil AS. Measurement of supercapacitor fractional-order model parameters from voltage-excited step response. *IEEE J Emerging Sel Top Circuits Syst* 2013;3(3):367–76.
- [18] Tsirimokou G, Pyschalinos C, Elwakil AS, Allagui A. Simple non-impedance-based measuring technique for supercapacitors. *Electron Lett* 2015;51(21):1699–701.
- [19] Radwan AG, Fouda M. Optimization of fractional-order RLC filters. *Circ Syst Signal Process* 2013;32(5):2097–118.
- [20] Radwan AG, Salama K. Passive and active elements using fractional  $L_{\mu}C_{\alpha}$  circuit. *IEEE Trans Circuits Syst I* 2011;58(10):2388–97.